


RESEARCH ARTICLE

Data for characterization of the optical properties of Atlantic salmon (*Salmo salar*) blood

Eirik Svendsen^{1,2}  | Lise L. Randeberg³ | Martin Føre¹ | Bengt Finstad⁴ | Rolf Erik Olsen⁴ | Nina Bloecher² | Jo Arve Alfredsen¹

¹Department of Engineering Cybernetics, Norwegian University of Science and Technology, Trondheim, Norway

²Department for Aquaculture, SINTEF Ocean AS, Trondheim, Norway

³Department of Electronic Systems, Norwegian University of Science and Technology, Trondheim, Norway

⁴Department of Biology, Norwegian University of Science and Technology, Trondheim, Norway

Correspondence

Eirik Svendsen, Department of Engineering Cybernetics, Norwegian University of Science and Technology, Trondheim, 7034, Norway.

Email: eirik.svendsen@sintef.no

Funding information

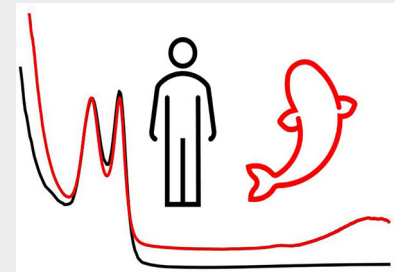
Norges Forskningsråd; SINTEF Ocean AS; Research Council of Norway, Grant/Award Number: 280864

Abstract

Photoplethysmography is a recent addition to physio-logging in Atlantic salmon which can be used for pulse oximetry provided that the properties for light propagation in salmon tissues are known.

In this work, optical properties of three

constituents of Atlantic salmon blood have been characterized using a photo spectrometer in the VIS–NIR range (450–920 nm). Furthermore, Atlantic salmon blood cell size has been measured using a Coulter counter as part of light scattering property evaluations. Results indicate that plasma contributes little to scattering and absorption for wavelengths typically used in pulse oximetry as opposed to blood cells which are highly scattering. Extinction spectra for oxygenated and deoxygenated hemoglobin indicate that Atlantic salmon hemoglobin is similar to that in humans. Pulse oximetry sensors originally intended for human applications may thus be used to estimate blood oxygenation levels for this species.



KEYWORDS

blood cells, extinction, hemoglobin, photoplethysmography, plasma, scattering, spectral analysis

1 | INTRODUCTION

The advent of miniaturized sensors for measurement of physiological signals has enabled wearable devices for use in, for example, patient monitoring [1], sports performance tracking [2] and animal monitoring [3]. Such devices have found their use in fishes as they can contribute to improved understanding of behavioral and physiological responses [4]. This is particularly relevant for Atlantic salmon (*Salmo salar*) as it is an important

species in aquaculture with 2.7 million tonnes live weight produced worldwide in 2020 [5].

Salmon husbandry entails a broad range of interrelated operations (e.g., feeding, crowding, pumping) with convoluted effects on (fish) stress level, welfare and mortality rates [6, 7]. For ethical and economic reasons such effects must be minimized. However, our current understanding of the behavioral and physiological responses of salmon to aquaculture operations is limited. Relevant physiological data must therefore be collected from

This is an open access article under the terms of the [Creative Commons Attribution](https://creativecommons.org/licenses/by/4.0/) License, which permits use, distribution and reproduction in any medium, provided the original work is properly cited.

© 2023 The Authors. *Journal of Biophotonics* published by Wiley-VCH GmbH.

individuals in different contexts so physiological tolerances can be better understood. Such extended knowledge can then be used to further refine and tailor Atlantic salmon husbandry operations to minimize stress, thus improving animal welfare [8, 9].

Measuring individual-level physiological data is commonly done using intraperitoneal implants [4]. The selection of parameters possible to acquire with this technique was recently expanded to include photoplethysmography (PPG) [10]. This facilitates more robust heart rate measurements [11] and, potentially, pulse oximetry (PO) for blood oxygen saturation (SpO_2) estimation—an interesting parameter to monitor in environments with variations in dissolved oxygen [12, 13]. Successful SpO_2 estimation, however, depends on knowledge of parameters determining light propagation in tissues [14]. While a large body of such data on mammalian tissues is available in literature (e.g., [15]), this is not the case for Atlantic salmon and fishes in general. In the context of PO, blood is a particularly important (fluid) tissue since knowledge of blood absorption and scattering characteristics largely determine the optical path length crucial for SpO_2 estimation [14, 16]. The purpose of this work was therefore to obtain data for characterization of the optical properties of Atlantic salmon blood in the visible to near-infrared (VIS–NIR) wavelength range, and to identify suitable procedures for obtaining such data. This will support future analysis of PPG data obtained from this species using any pulse oximeter with the aim to estimate SpO_2 .

To this end, blood was sampled from 10 fish in total. Five blood samples were used to extract plasma, hemoglobin and blood cells. The VIS–NIR spectra were then recorded for plasma and oxygenated and deoxygenated hemoglobin and blood cell solutions. The remaining five blood samples were used to measure cell sizes using a Coulter counter to support optical scattering evaluations.

2 | MATERIALS AND METHODS

2.1 | Ethics statement

During blood sampling all individuals were in surgical anesthesia (level 3 [17]). Blood sampling was approved under experiment animal permit 26 085 issued by the animal ethics committee of the Norwegian Food Safety Authority.

2.2 | Experiment animals

Atlantic salmon post smolt were held in an indoor tank ($2 \times 2 \times 1.6$ m) (SINTEF Ocean AS, Trondheim, Norway) supplied with 9°C filtered seawater (30 L per min) from

70 m depth. The tank was equipped with a Sterner Oxyguard oxygenation system maintaining oxygen saturation $\geq 85\%$, and a water circulation pump (EMAUX SuperPower) to maintain a current speed of 1 body length (BL) per at the tank periphery and 24 h lighting to stimulate growth. The fish were fed commercial feed (Skretting, 2 mm) at 2% of the tank biomass distributed across 12 feedings per 24 h using automatic feeders. In total, 10 fish (181 ± 56.5 g, 264 ± 25 mm, 1.26 ± 0.09 Fulton's condition factor [18]) were used for two main samplings: Spectral measurements (5 fish) and cell size measurements for light scattering evaluations (5 fish).

2.3 | Blood sampling

For blood sampling, a 1.10×38 mm (19G \times 1.5") needle was mounted on a 3 ml syringe. 5000 IU heparin was pulled into the syringe to coat and lubricate the inner walls. The syringe was then emptied by pushing the syringe's plunger to the hub. A random fish was captured from the holding tank using a knotless dip net and immediately transferred to a tub containing 70 mg/L Benzoak Vet knock-out anesthetic. When the fish was judged to have reached surgical anesthesia (level 3 [17]), it was placed ventral side up on a holding tray for blood sampling. Blood was sampled from the caudal vein/artery of the fish by inserting the needle in parallel with the sagittal plane posterior from the anal fin (i.e., the anterior region of the caudal peduncle). With the needle in place, ≥ 2 ml blood was drawn into the syringe. After removing the needle, the blood was transferred to a 6 ml Vacutainer tube coated with 1.8 mg per K2EDTA. The sample was then transferred to an 2 ml Eppendorf tube (or equally divided between two) for immediate processing in a room with a temperature of 15°C .

2.4 | Blood processing

2.4.1 | Plasma extraction

To obtain plasma, whole blood was centrifuged in its Eppendorf tube using a Hettich EBA 3S centrifuge (Hettich GmbH & Co. KG, Tuttlingen, Germany) at 1500 RPM / 195 g for 10 min. After centrifuging, the supernatant (plasma) was removed for spectral measurements using a pipette.

2.4.2 | Blood cell extraction

To obtain blood cell samples, the packed cell volume remaining after plasma removal was washed by adding

1 ml Phosphate Buffered Saline (PBS) (137 mmol) to the packed cell volume (PCV) in the Eppendorf tube after plasma extraction. The mix was then centrifuged at 1500 RPM/195 g for 1 min. The supernatant was removed using a pipette and discarded. This procedure was repeated twice. The relatively gentle centrifuging compared with other protocols (e.g., [19]) was necessary because previous attempts showed that applying greater force to the samples resulted in increased hemolysis and a PCV which did not dissolve in PBS during cell washing. This also excluded the use of plasma separator Vacutainers which requires powerful centrifuging for the cells to pass through the separating gel. 25 μ l of the PCV remaining after the second wash were then pipetted into a test tube containing 50 ml PBS and carefully agitated for mixing to obtain a 1:2000 ratio. This sample was divided into equal parts and 25 ml PBS added to obtain two times 25 ml samples in a 1:4000 ratio.

2.4.3 | Hemoglobin extraction

Hemoglobin was extracted from blood cells by pipetting 50 μ l of the PCV after washing into a test tube containing 50 ml deionized water resulting in a ratio of 1:250. The tube was then capped, agitated to promote hemolysis and finally divided equally between two test tubes for further processing and analysis.

2.4.4 | Sample oxygenation and deoxygenation

Samples (1:4000 blood cells+PBS or 1:250 hemoglobin +deionized water) were oxygenated or deoxygenated via gassing using industrial oxygen (purity \geq 99%) or instrument nitrogen (purity \geq 99.9%), respectively. Gassing was achieved using closed test tubes with gas tight penetrations. A 0.5 \times 25 mm (25G \times 1") needle was inserted through the cap and glued in place for pressure relief (Figure 1). All samples were gassed for \geq 20 min since shorter gassing times resulted in large differences in the measured spectra.

2.5 | Spectral measurements

2.5.1 | Sensing equipment

Spectral data were collected using a Flame FLAME-T-VIS-NIR-ES (350–1000 nm) spectrometer and a 360–2000 nm HL-2000-LL tungsten-halogen light source. The spectrometer and light source were connected to a SQUARE ONE cuvette holder via a QP200-2-VIS-NIR fiber

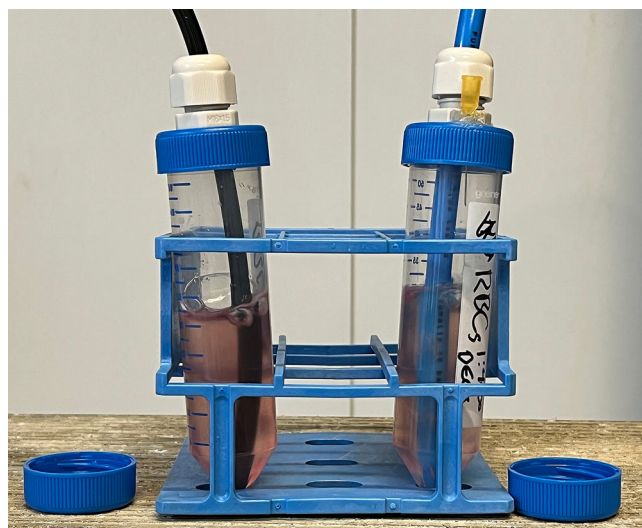


FIGURE 1 Sample gassing set up. Note that the sample volume in the left test tube is lower compared with the right because a sample had been removed from the tube before the image was taken.

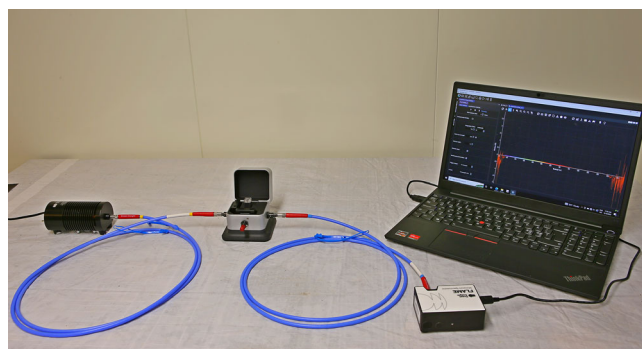


FIGURE 2 Sensing equipment. From left to right: Light source, cuvette holder, spectrometer, and laptop.

(200 μ m core diameter) on the source side, and a QP50-2-VIS-NIR fiber (50 μ m core diameter) on the detector side. All equipment from Ocean Insight, Duiven, The Netherlands. The light source was allowed a \geq 30 min warm-up time for it to reach thermal equilibrium with the environment to minimize drift. The spectrometer was controlled using OceanView (v2.0.7) by OceanInsight (Ocean Insight, Duiven, The Netherlands) running on a Leonovo laptop. All samples were measured using a CVS-Q-10 quartz cuvette with a 10 mm path length and a 1.4 ml maximum sample volume. The set-up is shown in Figure 2.

By adding a sample to the cuvette, this set up allows measurement of the sample's extinction, that is, its combined absorption and scattering spectrum [20]. Before each spectral measurement, the cuvette was flushed with PBS and its outside wiped with 96% ethanol using a

non-lint cloth. The spectrometer was then zeroed/reset by measuring the white and dark references using the cuvette filled with PBS.

By adding individual blood constituents to the cuvette, knowledge on the optical properties could be obtained. Spectra were measured for five undiluted plasma samples, oxygenated and de-oxygenated 1:4000 washed blood cells+PBS samples and oxygenated and deoxygenated 1:250 hemoglobin+deionized water samples, respectively. A measurement was defined as the average of 200 scans acquired using 750 μ s integration time, with a boxcar width of 10. Both electric dark and non-linearity corrections were enabled.

For the purpose of visual comparison, all samples were photographed using a tripod-mounted Canon EOS-1D X, 18.1 megapixel full-frame DSLR camera with a Canon 70–200 f/2.8 L IS II USM lens. The lens was set to 200 mm and the aperture to f/2.8 to maximize background separation. All images were captured against an even, white background and included a calibrated 18 gray reflectance standard for color and intensity corrections. Color and intensity corrections were done as post-processing using GNU Image Manipulation Program (GIMP) V2.10. Following color and intensity corrections, the cuvette was cut from the image. All sample images are given in Data S1.

2.6 | Cell size measurement and whole blood scattering coefficient

To estimate a value for the whole blood scattering parameter, μ_s , published values for blood cell prevalence and volume for Atlantic salmon blood were compiled (Table 2). Using the average of the compiled data, values for particle concentration per μm^3 and spherical-equivalent diameters in μm were calculated. The particle concentration was found by dividing the average number of blood cells per L by 10^{15} which is the number of μm^3 per L. The spherical-equivalent diameter, D_{cell} , was found by using the average blood cell volume, V_{cell} inserted into the expression for sphere volume and solving for the radius, r_{cell} , so

$$D_{\text{cell}} = 2 \cdot r_{\text{cell}} = 2 \cdot \left(\sqrt[3]{\frac{3V_{\text{cell}}}{4\pi}} \right). \quad (1)$$

With these values, μ_s was calculated for 660, 880, and 940 nm using Prah's Mie scattering calculator [21]. These are wavelengths commonly used in pulse oximetry and are therefore of particular interest to facilitate this sensing technique for Atlantic salmon.

Measurements in the five last blood samples were obtained by subjecting the samples to the same procedure of plasma removal and cell washing as described above. The resulting samples were then diluted in PBS in a 1:800000 ratio before their spherical equivalent sizes were measured using a Coulter counter (Multisizer 4, Beckman Coulter, South Kraemer Boulevard, Brea, California 92821-6232) with a 100 μm aperture. Each measurement was the average of three runs on the same sample (i.e., fish) by the Coulter counter. The resulting cell sizes were compared with those computed from published data to assess that these were similar.

3 | RESULTS AND DISCUSSION

3.1 | Spectral measurements

The measured plasma extinction spectra are shown in Figure 3.

The plasma samples were clear to the naked eye but with slight differences in hue (see Data S1). The average plasma extinction spectrum showed two small peaks at 540 and 576 nm typically associated with oxyhemoglobin, thus indicating its presence in the samples and possibly explaining the differences seen in sample color.

The plasma spectra showed low extinction between 500 and 820 nm and increasing extinction outside this range. This is similar to spectra reported for human blood [22], and may be caused by plasma protein scatterers in the low end of the spectrum and increasing absorption by water in the higher end. Because PO use wavelengths where plasma extinction is low, special considerations for plasma effects are likely unnecessary when estimating SpO_2 .

Washed blood cell extinction spectra are presented in Figures 4 and 5.

The blood cell extinction spectra are similar in morphology compared with those reported for human blood cells [23] within the measured wavelength range. As seen in Figure 5, deoxygenated blood cells display slightly lower extinction values below 840 nm.

The averaged extinction spectrum for oxygenated blood cells had two peaks at 540 and 576 nm, respectively, which are associated with oxyhemoglobin. The absence of these peaks in the spectrum for deoxygenated blood cells indicates that the gassing approach was effective. The noise in the far ends of the measured range can be attributed to the HL-2000-LL tungsten-halogen light source being weaker for these wavelengths, thus reducing the signal to noise ratio. Also note that the measured extinction for the blood cell dilution is higher compared

FIGURE 3 Extinction spectra for undiluted plasma. The black line illustrates the average for all samples, while the colored background illustrates the min-max range within which individual plasma spectra were distributed.

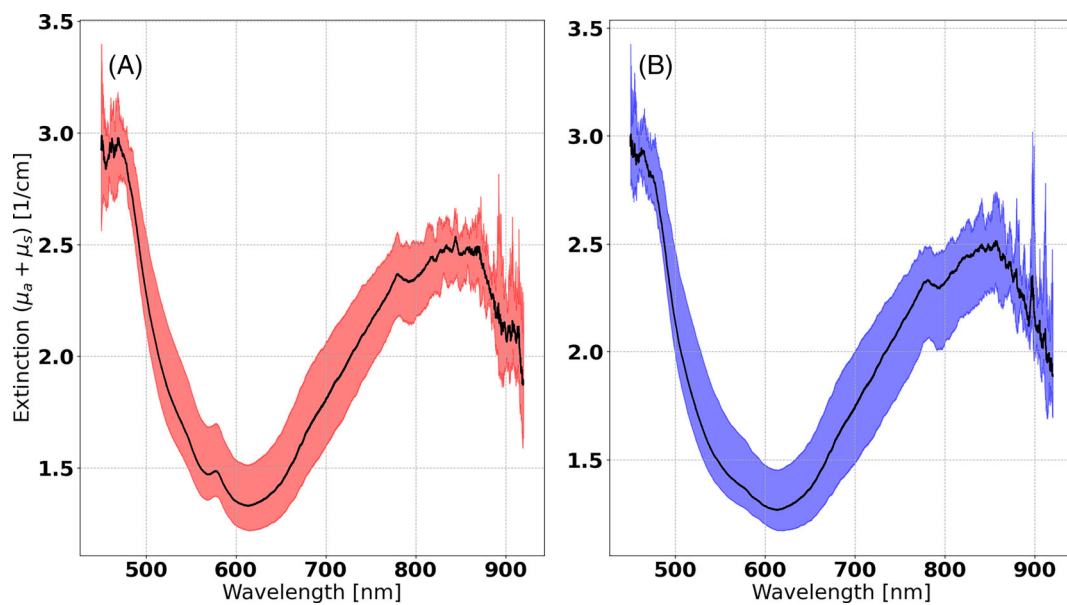
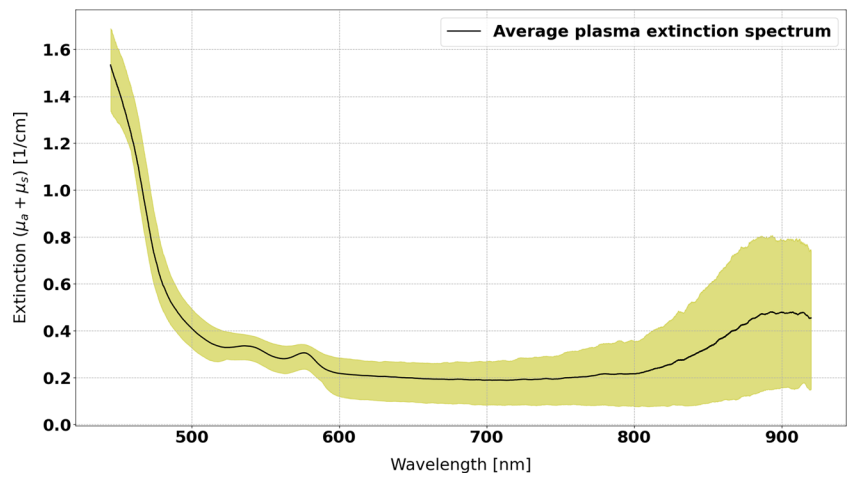
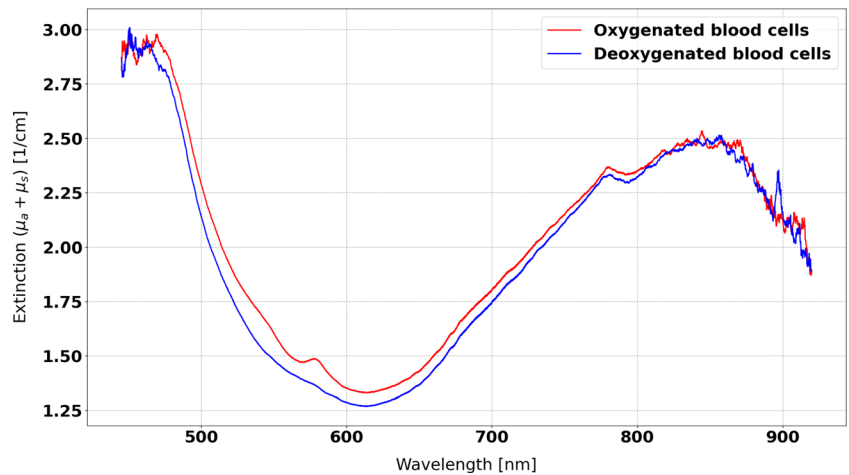


FIGURE 4 Extinction spectra for (A) oxygenated and (B) deoxygenated blood cells in a 1:4000 PBS dilution. The solid black lines are the mean of all measured samples, while the colored backgrounds illustrate the min-max range within which individual spectra were distributed.

FIGURE 5 Comparison of blood cell extinction spectra in a 1:4000 PBS dilution. The solid red line is the mean of all measured samples of oxygenated blood cells while the solid blue line is the mean of all measured samples of deoxygenated blood cells.



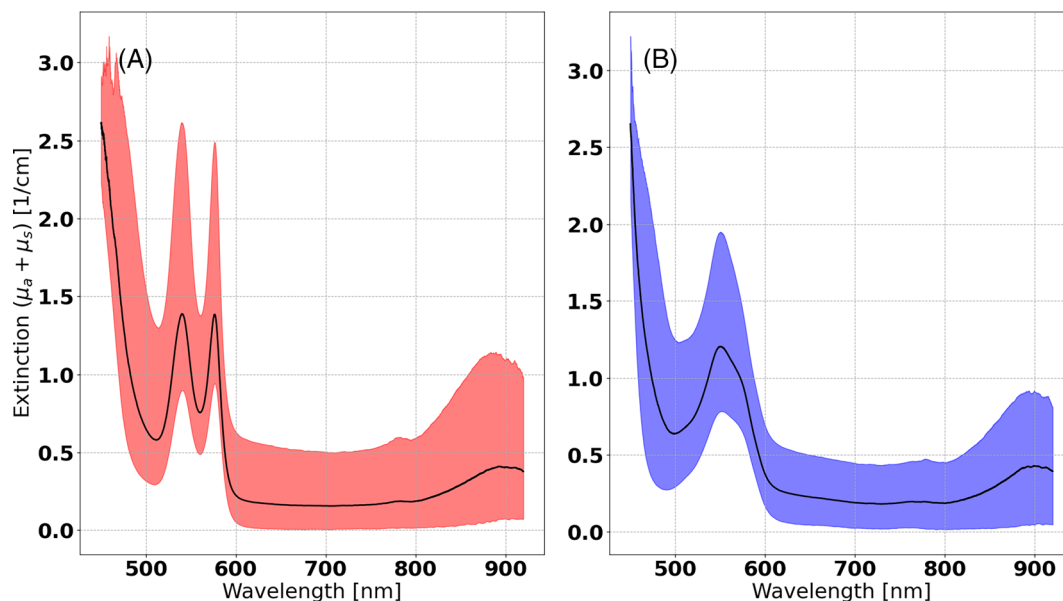


FIGURE 6 Extinction spectra using 1:250 deionized water dilutions for (a) oxyhemoglobin with spectral peaks at 540 and 576 nm and (b) deoxyhemoglobin with a spectral peak at 550 nm. The solid black lines are the mean values, while the colored backgrounds illustrate the min-max range within which individual spectra were distributed.

with plasma (Figure 3 vs. Figure 4). This indicates that Atlantic salmon blood cells are highly scattering.

Oxyhemoglobin and hemoglobin extinction spectra were expected to be dominated by absorption. The extinction spectrum for the former showed two distinct spectral peaks at 540 and 576 nm (Figure 6A), while the extinction spectrum for the latter showed a spectral peak at 550 nm (Figure 6B).

The averaged hemoglobin spectrum exhibited the expected morphology up to 850 nm. Beyond this wavelength, an unexpected isosbestic point was identified. This can be explained by the properties of the HL-2000-LL tungsten-halogen light source which is weak in the far ends of the measured wavelength range. The resulting reduction in signal to noise ratio will therefore affect accuracy in these regions if extinction is low. This effect was minimized by using an appropriate sample concentration (1:4000 for blood cells and 1:250 for hemoglobin), high averaging (200 samples) and integration time (750 μ s). It is, however, generally difficult to achieve 0% and 100% oxygenation levels. The samples may therefore have been close to, but not completely at, these levels. Furthermore, any remaining cells and scatterers in the samples would also have introduced a scattering component in the measurement adding to the effect (Figure 7).

Sample transfer was achieved by pipetting directly from the gassing test tube into the measurement cuvette. Apart from the opening at the tip, the pipette was completely closed. Transfer of the sample to the cuvette

and spectral measurement was achieved within a matter of seconds. Although this method momentarily exposed the samples to air after transfer to the cuvette, consistent results were obtained using 200 samples and 750 μ s for averaging and integration time, respectively. The method was, thus, considered sufficiently robust for the purpose of this work. Future attempts at such measurements may consider using a completely closed sample transfer system, for example, by integrating a sampling tube in the gassing system.

The measured spectra and published spectra for human hemoglobin [24] were scaled to the value of their first spectral peak (540 nm for Atlantic salmon and human oxyhemoglobin, 550 nm for Atlantic salmon hemoglobin and 555 nm for human hemoglobin, respectively) and plotted for comparison (Figure 8).

Atlantic salmon hemoglobin spectra presented in Figure 8 show a morphology similar to human hemoglobin. Although the spectra for salmon oxyhemoglobin and deoxyhemoglobin were expected to be dominated by absorption some degree of scattering must be expected. Since the human oxyhemoglobin and hemoglobin spectra are considered to be reference absorption spectra they are virtually unaffected by scattering, thus leading to differences in morphology. It is also noted that the oxyhemoglobin spectrum (Figure 8A) has a small peak at 757 nm. This peak is typical for hemoglobin which indicates that the samples were not fully oxygenated, adding to the divergence from the (human) reference.

FIGURE 7 Comparison of average oxyhemoglobin (red) and deoxyhemoglobin spectra (blue) in a 1:250 deionized water dilution. The blue dots denote the isosbestic points (i.e., crossings).

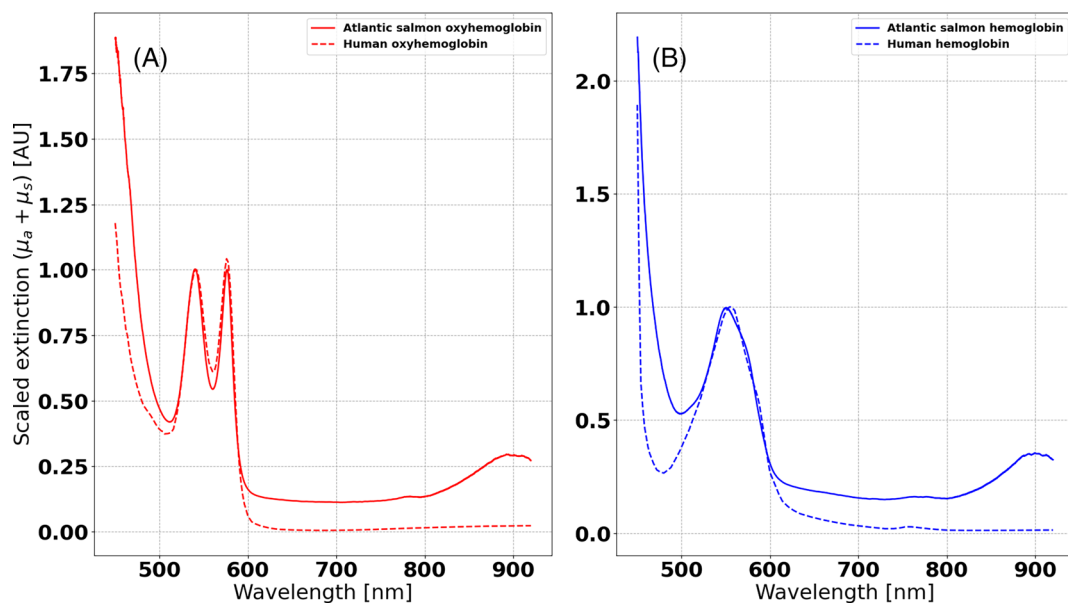
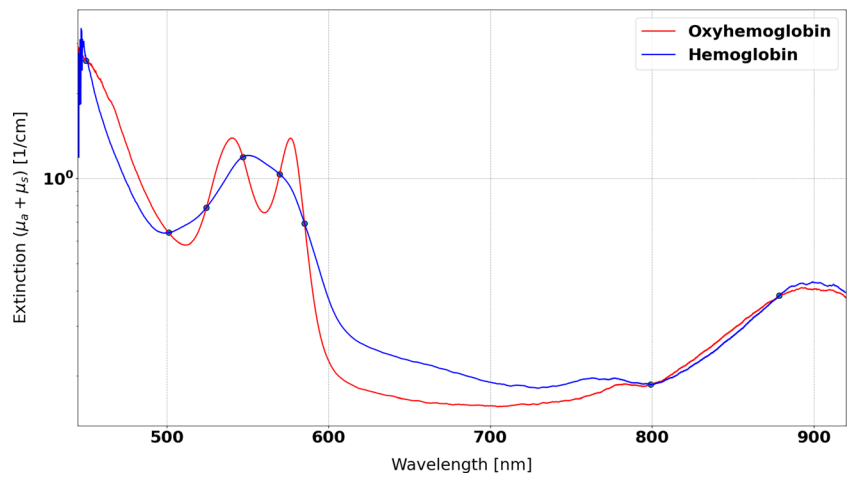


FIGURE 8 Comparison of measured Atlantic salmon and human scaled oxyhemoglobin (A) and hemoglobin (B) spectra. Due to the scaling, values along the y-axis are given in arbitrary units (AU).

Using the hemoglobin extinction spectra, a list of points with equal extinction (i.e., isosbestic points) can be compiled and compared with reference values for human hemoglobin [24].

Table 1 shows that the isosbestic points for Atlantic salmon hemoglobin are very close to those reported for human hemoglobin. The differences may be introduced by residual scatterers in the samples. Note also that the abovementioned unexpected isosbestic point at 879 does not have a counterpart in human blood.

The Coulter counter measurements (Figure 9) show two distinct peaks for spherical equivalent diameters of 7.2 and 8.84 μm indicating that the washed cell samples contained two dominating cell populations.

Since washing mainly removes plasma, the remaining PCV must be expected to include multiple cell types

typically found in Atlantic salmon blood, such as erythrocytes, reticulocytes, white blood cells (e.g., neutrophils, monocytes, and lymphocytes) and platelets (thrombocytes). Out of these, erythrocytes were expected to dominate in size and number ($\approx 1 \times 10^{12} \cdot \text{L}^{-1}$) [25, 26] followed by reticulocytes (smaller, immature erythrocytes) constituting $\approx 15\%$ of all blood cells [26, 27]. This mix of cell sizes and prevalence is a likely contributor for the two peaks seen in Figure 9. Another potential impact is that Coulter counter size estimates depend on a range of factors such as particle shape and lateral position when passing through the counter's aperture. Thus, due to the oblate shape of Atlantic salmon blood cells, their orientation as they pass through the aperture will affect the size estimate. The two most extreme orientations “flat” and “on edge” may therefore contribute to separate the

measurement into two distinct peaks [28] as seen in the results. To reduce this effect, the Coulter counter aperture was ≈ 10 times larger than the largest expected particle size as recommended for such measurements. Nevertheless, the combination of this effect and the mix of cell sizes is considered a likely explanation for this result.

The peak for the largest particle size (8.84 μm) from the Coulter counter results was assumed to represent the spherical equivalent blood cell diameter. This value was compared with published values to evaluate the blood sample quality and assess other unmeasured parameters (Table 2).

The spherical equivalent cell diameter obtained from the Coulter counter measurements were consistent with published values, indicating that the blood samples used in this work were representative for Atlantic salmon blood. This also indicates that all fish used for blood sampling in this work were in good health.

Since the cell sizes in Table 2 are orders of magnitude larger than the wavelengths used in the spectral measurements, Mie scattering is dominant [20]. In Mie scattering,

TABLE 1 Isosbestic points for Atlantic salmon compared with human hemoglobin.

Atlantic salmon hemoglobin	Human hemoglobin
450	452
501	500
525	529
547	545
570	570
585	584
799	797
879	–

scattering efficiency increases with the fourth power of the particle size [16] which means that the largest particles contribute more to scattering than smaller particles. The peak for the cell population with the largest diameter was therefore used to calculate μ_s .

Mie scattering calculations depend on the refractive index of both the medium (i.e., plasma) and the spheres (i.e., the blood cells) [20]. To the best of the authors knowledge, no published values for refractive indices for Atlantic salmon blood have been published. It was therefore assumed that Atlantic salmon blood has refractive indices similar to those published for human blood [31, 32]. Using the average values in Table 2 and these refractive indices as input to the Mie calculator [21] for selected wavelengths used in pulse oximetry, we obtain the scattering parameter values in Table 3.

The values for μ_s obtained using these methods are larger than those published for human blood [33]. This was expected and is consistent with Mie scattering theory because Atlantic salmon blood cells are larger compared with those in humans.

TABLE 2 Overview of literature values listing cell density as cells per, cell volume as mean corpuscular volume (MCV, μm^3), and cell diameter (D) calculated using Equation (1), as well as the average of those values compared with the result from this study.

C (cells/ μl)	MCV (μm^3)	D (μm)	References
$0.97 \cdot 10^{-3}$	485	9.75	[25]
$0.97 \cdot 10^{-3}$	369	8.90	[29]
$0.83 \cdot 10^{-3}$	489	9.77	[30]
$1.25 \cdot 10^{-3}$	366	8.87	[26]
$1.29 \cdot 10^{-3}$	324	8.52	[27]
–	362	8.84	Coulter counter
$1.01 \cdot 10^{-3}$	399	9.23	Average

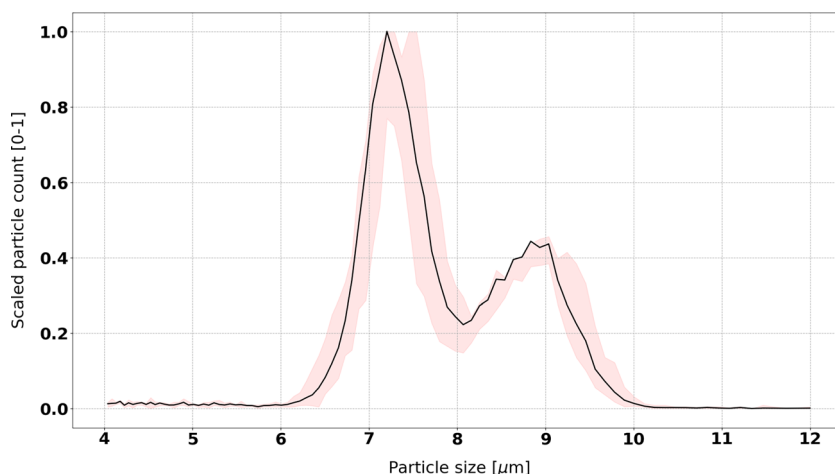


FIGURE 9 Coulter counter results of measured cell size. The solid black line shows the average of all measurements, while the colored background illustrates the min-max range of the measurements.

TABLE 3 Estimated scattering coefficient, μ_s , for Atlantic salmon whole blood for selected wavelengths used in pulse oximetry.

λ (nm)	μ_s (cm ⁻¹)
660	1887
880	2207
940	2170



FIGURE 10 Example of plasma sample with hemolysis typically observed after vacutainer blood sampling (A) compared with plasma obtained using syringes (B).

3.2 | Sampling challenges

The blood sampling and processing methods described in Materials and methods are the final result of multiple attempts to measure optical properties of Atlantic salmon blood because preceding attempts presented several challenges which had to be overcome.

Two main methods for blood sampling were compared: Using syringes and Vacutainers. The latter is attractive due to the ease of sampling and the wide selection of available anti-coagulant coatings as well as plasma

separator gels. Processing of samples obtained using Vacutainers, however, consistently resulted in various degrees of hemolysis evident in the form of red-tinted plasma as shown in Figure 10.

Consequently, it was decided to use heparinized syringes and 19G needles. Even then, oxygen peaks were present in measured plasma absorption spectra (Figure 3) indicating some hemolysis taking place during sampling.

Hemolysis of blood cell dilutions also occurred during gassing if bubbling was too vigorous. The latter was seen when attempting to improve gas distribution in samples using an air stone (sinter) even at the lowest gas pressure available equipment would allow. This was likely caused by turbulence in the gap between the air stone and the test tube wall resulting in shear forces excessive for cell integrity. Bubbling was, thus, changed to using gas tubing directly in the samples (Figure 1).

During earlier tests, sample deoxygenation was attempted using sodium dithionite. Dosing was according to [34] without achieving consistent results. Samples were either not deoxygenated within the expected time frame or rapidly started to form methemoglobin [35]. Future attempts to deoxygenate dilutions of salmon blood constituents should therefore be preceded by a systematic study on how to obtain consistent and reliable deoxygenation using sodium dithionite.

Some of the measured hemoglobin solutions contained impurities (see Data S1). The light passes through the sample slightly below middle height of the cuvette. Because all samples were clear/homogeneous to the naked eye in this area, such contamination is considered to have had limited effect on the results. Nevertheless, future attempts at measuring the optical properties of salmon blood may consider filtering the hemoglobin samples using, for example, a nylon mesh before gassing and measurement.

Sample coagulation was also a challenge. Despite using heparin in vessels during blood collection, samples would (partially) coagulate before centrifuging if left unprocessed on the rocker for more than approximately 30 min. Additionally, samples obtained using only heparin coagulated rapidly when adding deionized water to obtain the hemoglobin solution. These events may be explained by the onset of the coagulation cascade. At some point the amount of heparin present in the sample can no longer block fibrin formation during hemolysis and the sample coagulates. The addition of K2EDTA to the samples prevented these issues, likely by blocking calcium. In the future, sodium citrate may be tested as an alternative directly in the syringe since it acts as both an anti-coagulant and a calcium blocker if an acceptable mixing ratio can be identified.

4 | CONCLUSION

This work presents data describing the optical properties of Atlantic salmon blood between 450 and 920 nm. This wavelength range is relevant for pulse oximetry sensors which typically use wavelengths around 660, 880, and 940 nm.

The results indicate that plasma contributes little to scattering and absorption, which hemoglobin absorption is similar to that in humans and that blood cells have strong scattering properties. Furthermore, a novel sampling procedure had to be established to obtain these measurements, as no suitable methods for such sampling on fish blood existed. This method can be used and further refined for future measurements of blood from salmon and other fishes, and is as such a contribution to the toolbox available for science.

In the context of pulse oximetry, the low plasma absorbance indicates that plasma will not require special compensation when aspiring to sample SpO_2 . Furthermore, the isosbestic points for hemoglobin absorbance imply that published values for molar extinction coefficients for human hemoglobin and oxyhemoglobin [24] can be used, thus supporting that pulse oximeters originally intended for human applications can be used for similar purposes in Atlantic salmon. However, scattering results show that Atlantic salmon blood is highly scattering, thus implying that PPGs obtained by a pulse oximeter must be compensated. This can be achieved using the scattering parameters in Table 3 as part input to the pulse oximeters SpO_2 estimation algorithm. Accurate SpO_2 estimation may increase understanding of the physiological responses and tolerances of Atlantic salmon via scientific trials using raceways or swim tunnels where water quality can be controlled and stress levels accurately quantified. Using such knowledge, SpO_2 estimation in Atlantic salmon farming may, thus, facilitate adaptation of production methods for stress reduction and improved animal welfare.

ACKNOWLEDGMENT

This work was carried out as part of the SalmonInsight project funded by the Research Council of Norway (project number 280864) and through in-kind provided by SINTEF Ocean AS.

CONFLICT OF INTEREST STATEMENT

The authors declare no conflict of interest.

DATA AVAILABILITY STATEMENT

The data supporting the findings of this study are available from the corresponding author upon reasonable request.

ORCID

Eirik Svendsen  <https://orcid.org/0000-0003-1038-6560>

REFERENCES

- [1] J.-W. Jeong, W. Lee, Y.-J. Kim, *Sensors* **2021**, *22*, 104.
- [2] E. A. Thomson, K. Nuss, A. Comstock, S. Reinwald, S. Blake, R. E. Pimentel, B. L. Tracy, K. Li, *J Sports Sci* **2019**, *37*, 1411.
- [3] H. J. Williams, J. Ryan Shipley, C. Rutz, M. Martin Wikelski, L. A. H. Wilkes, *Philos Trans Roy Soc B* **2021**, *376*, 20200230.
- [4] E. B. Thorstad, A. H. Rikardsen, A. Alp, F. Økland, *Turk J Fish Aquat Sci* **2013**, *13*, 881.
- [5] FAO. Food and Agriculture Organization of the United Nations, Fisheries and Aquaculture Department. **2022** https://www.fao.org/fishery/statistics-query/en/aquaculture/aquaculture_quantity
- [6] C. Noble, K. Gismervik, M. H. Iversen, J. Kolarevic, J. Nilsson, L. H. Stien, J. F. Turnbull, *Welfare Indicators for farmed Atlantic salmon: tools for assessing fish welfare*, Nofima, Tromsø, Norway **2018**.
- [7] I. Sommerset, B. B. Jensen, G. Bornø, A. Haukaas, E. Brun, *Fiskehelse rapporten*, Norwegian Veterinary Institute, Ås, Norway **2021**.
- [8] M. Føre, K. Frank, T. Norton, E. Svendsen, J. A. Alfredsen, T. Dempster, H. Eguiraun, W. Watson, A. Stahl, L. M. Sunde, C. Schellewald, K. R. Skoien, M. O. Alver, D. Berckmans, *Biosyst Eng* **2018**, *173*, 176.
- [9] M. Føre, K. Frank, T. Dempster, J. A. Alfredsen, E. Høy, *Aquacult Eng* **2017**, *78*, 163.
- [10] E. Svendsen, M. Føre, L. L. Randeberg, J. A. Alfredsen, *IEEE Sens* **2021**, *1*, 4.
- [11] E. Svendsen, F. Økland, M. Føre, L. L. Randeberg, B. Finstad, R. E. Olsen, J. A. Alfredsen, *Anim Biotelemetry* **2021**, *9*, 1.
- [12] M. O. Alver, M. Føre, J. A. Alfredsen, *Aquaculture* **2022**, *548*, 737720.
- [13] D. Johansson, K. Ruohonen, A. Kiessling, F. Oppedal, J.-E. Stiansen, M. Kelly, J.-E. Juell, *Aquaculture* **2006**, *254*, 594.
- [14] P. A. Kyriacou, J. Allen, *Photoplethysmography: Technology, Signal Analysis and Applications*, Academic Press, London **2021**.
- [15] J. L. Sandell, T. C. Zhu, *J Biophoton* **2011**, *4*, 773.
- [16] I. J. Bigio, S. Fantini, *Quantitative biomedical optics: theory, methods, and applications*, Cambridge University Press, Cambridge **2016**.
- [17] S. D. Coyle, R. M. Durborow, J. H. Tidwell, et al., *Anesthetics in Aquaculture*, Vol. 3900, Southern Regional Aquaculture Center Stoneville, Stoneville **2004**.
- [18] W. E. Ricker, *Bull. Fish. Res. Bd. Can.* **1975**, *191*, 1.
- [19] M. Iversen, B. Finstad, R. S. McKinley, R. A. Eliassen, K. T. Carlsen, T. Evjen, *Aquaculture* **2005**, *243*, 373.
- [20] C. F. Bohren, D. R. Huffman, *Absorption and Scattering of Light by Small Particles*, John Wiley & Sons, New Jersey **1983**.
- [21] S. Prah. Mie scattering calculator. **2018** https://omlc.org/calc/mie_calc.html
- [22] M. Meinke, G. Müller, J. Helfmann, M. Friebel, *J Biomed Opt* **2007**, *12*, 014024.

- [23] M. Friebel, J. Helfmann, U. Netz, M. Meinke, *J Biomed Opt* **2009**, *14*, 034001.
- [24] S. Prah. Optical Absorption of Hemoglobin. **1999** <https://omlc.org/spectra/hemoglobin/>
- [25] K. Sandnes, Ø. Lie, R. Waagbø, *J Fish Biol* **1988**, *32*, 129.
- [26] K. Hamre, B. Hjeltnes, H. Kryvi, S. Sandberg, M. Lorentzen, Ø. Lie, *Fish Physiol. Biochem.* **1994**, *12*, 421.
- [27] J. Härdig, L. B. Höglund, *Comp Biochem Physiol A Physiol* **1983**, *75*, 35.
- [28] Z. Qin, J. Zhe, G.-X. Wang, *Meas. Sci. Technol.* **2011**, *22*, 045804.
- [29] J. Sadler, R. M. G. Wells, P. M. Pankhurst, N. W. Pankhurst, *Aquaculture* **2000**, *184*, 349.
- [30] H. D. Rodger, R. H. Richards, *J Fish Dis* **1998**, *21*, 101.
- [31] N. Ghosh, P. Buddhiwant, A. Uppal, S. K. Majumder, H. S. Patel, P. K. Gupta, *Appl. Phys. Lett.* **2006**, *88*, 084101.
- [32] S. Liu, Z. Deng, J. Li, J. Wang, N. Huang, R. Cui, Q. Zhang, J. Mei, W. Zhou, C. Zhang, et al., *J Biomed Opt* **2019**, *24*, 035003.
- [33] N. Bosschaart, G. J. Edelman, M. C. G. Aalders, T. G. van Leeuwen, D. J. Faber, *Lasers Med Sci* **2014**, *29*, 453.
- [34] K. Briely-Sabo, A. Bjornerud, *Proc. Intl. Sot. Mag. Reson. Med* **2000**, *8*, 2025.
- [35] K. Dalziel, J. R. P. O'Brien, *Biochem. J.* **1957**, *67*, 119.

SUPPORTING INFORMATION

Additional supporting information can be found online in the Supporting Information section at the end of this article.

How to cite this article: E. Svendsen, L. L. Randeberg, M. Føre, B. Finstad, R. E. Olsen, N. Bloecher, J. A. Alfredsen, *J. Biophotonics* **2023**, *16*(9), e202300073. <https://doi.org/10.1002/jbio.202300073>